IJC Heart & Vasculature 40 (2022) 101029

Contents lists available at ScienceDirect

IJC Heart & Vasculature

journal homepage: www.sciencedirect.com/journal/ijc-heart-and-vasculature

# Patterns of cardiovascular magnetic resonance inflammation in acute myocarditis from South Asia and Middle East

Abdel-Nasser Ghareeb [a], Sabir A. Karim [a], Vivek P. Jani [b], Willington Francis [a], Jef Van den Eynde [b,c], Maryam Alkuwari [a], Shelby Kutty [b,*]

[a] Department of Clinical Imaging, Heart Hospital, Hamad Medical Corporation, Doha, Qatar
[b] Helen B. Taussig Center, The Johns Hopkins Hospital and School of Medicine, Baltimore, MD, USA
[c] Department of Cardiovascular Sciences, KU Leuven, Belgium

ARTICLE INFO

*Keywords:*
Viral myocarditis
Cardiovascular magnetic resonance
Global health
Machine learning
T1/T2 parametric mapping

ABSTRACT

*Background:* Cardiovascular magnetic resonance (CMR) is the test of choice for diagnosis and risk stratification of myocardial inflammation in acute viral myocarditis. The objective of this study was to assess patterns of CMR inflammation in a cohort of acute myocarditis patients from Northern Africa, Asia, and the Middle East using unsupervised machine learning.

*Methods:* A total of 169 racially and ethnically diverse adults (≥18 years of age) with CMR confirmed acute myocarditis were studied. The primary outcome was a combined clinical endpoint of cardiac death, arrhythmia, and dilated cardiomyopathy. Machine learning was used for exploratory analysis to identify patterns of CMR inflammation.

*Results:* Our cohort was diverse with 25% from Northern Africa, 33% from Southern Asia, and 28% from Western Asia/the Middle East. Twelve patients met the combined clinical endpoint – 3 had arrythmia, 8 had dilated cardiomyopathy, and 1 died. Patients who met the combined endpoint had increased anterior ($p = 0.034$) and septal ($p = 0.042$) late gadolinium enhancement (LGE). Multivariable logistic regression, adjusted for age, gender, and BMI, found that patients from Southern Asia ($p = 0.041$) and the Middle East ($p = 0.043$) were independently associated with lateral LGE. Unsupervised machine learning and factor analysis identified two distinct CMR patterns of inflammation, one with increased LGE and the other with increased myocardial T1/T2.

*Conclusions:* We found that anteroseptal inflammation is associated with worsened outcomes. Using machine learning, we identified two patterns of myocardial inflammation in acute myocarditis from CMR in a racially and ethnically diverse group of patients from Southern Asia, Northern Africa, and the Middle East.

## 1. Introduction

The global incidence of acute, infectious myocarditis is approximately 1.5 million cases per year, with most affected patients being young and healthy [1]. Unfortunately, there exist large disparities in outcomes regionally. In European countries, Canada, and the United States age-standardized disability-adjusted life years (DALYs) are 0–11 per 100,000 cases of acute myocarditis, while in Asia, Eastern Europe, and South America, DALYs are 54 per 100,000 cases [1]. The clinical manifestations of acute myocarditis are heterogeneous and range from subclinical disease to sudden cardiac death, new onset arrythmia, precordial chest pain, and syncope, often times in the setting of a viral prodrome [2]. As such, diagnosis remains challenging. The gold standard for diagnosis is endomyocardial biopsy (EMB) with histopathological evidence of myocardial inflammation. EMB is infrequently performed, however, because of perceived risks and low sensitivity of

*Abbreviations:* BSA, Body Surface Area; CMR, Cardiovascular Magnetic Resonance; CMV, Cytomegalovirus; CRP, C Reactive Protein; DALY, Disability-Adjusted Life Years; EBV, Epstein-Barr Virus (EBV); EGE, Early Gadolinium Enhancement; EMB, Endomyocardial Biopsy; HBV, Hepatitis B Virus; Hs, High-Sensitivity; IQR, interquartile range; LGE, Late Gadolinium Enhancement; LLC, Lake Louise Criteria; LVEDVi, Left Ventricular End Diastolic Volume indexed; LVEF, Left Ventricular Ejection Fraction; LVESVi, Left Ventricular End Systolic Volume indexed; RVEF, Right Ventricular Ejection Fraction; SD, Standard Deviation; T1, Spin-lattice relaxation; T2, Transverse relaxation.

* Corresponding author at: Helen B. Taussig Heart Center, The Johns Hopkins University School of Medicine, M2315, 1800 Orleans St, Baltimore, MD 21287, USA.
*E-mail address:* skutty1@jhmi.edu (S. Kutty).

https://doi.org/10.1016/j.ijcha.2022.101029
Received 19 March 2022; Accepted 4 April 2022

diagnostic criteria [3]. Consequently, cardiovascular magnetic resonance (CMR) has now evolved as the test of choice for diagnosis and risk stratification of acute myocarditis, as it is non-invasive with well-established criteria and reasonable sensitivity and specificity [4–7].

Recently, the incorporation of parametric T1 and T2 mapping have further improved the diagnostic accuracy of CMR for acute myocarditis [8–10]. Broadly, T2 mapping allows for quantification of myocardial edema [11], while T1 mapping and late gadolinium enhancement (LGE) allow for assessment of non-ischemic myocardial injury. Indeed, a 2018 update to the Lake Louise Criteria (LLC) for CMR-based diagnosis of acute myocarditis has improved sensitivity and specificity to 88% and 96%, respectively [12]. Furthermore, new guidelines for CMR in non-ischemic myocardial inflammation from 2018 detail the added benefit of T1 and T2 mapping in conjunction with early (EGE) and late (LGE) gadolinium enhancement. Edema sensitivity by T2 mapping is further suspected to correlate with differences in viral genomes, highlighting the idea that different patterns of CMR inflammation depend on the etiology of viral myocarditis [11,13,14].

As outcomes viral myocarditis vary globally, the objective of this study was to classify patterns of myocardial inflammation in a cohort of acute viral myocarditis patients from the Southern Asia and the Middle East. We first performed subgroup analysis by geography, gender, and age to identify differences in LGE, T1, and T2 parametric maps in this cohort of patients. We next sought to link these differences with specific demographic factors using multivariable logistic regression. Finally, we utilized Bayesian factor analysis in conjunction with unsupervised machine learning to agnostically classify patterns of CMR inflammation in this patient cohort.

## 2. Methods

### 2.1. Study patients and data collection

We retrospectively studied 169 consecutive adult patients (>18 years of age) admitted between April 2015 and December 2019 to Heart Hospital, Hamad Medical Corporation, Qatar, due to acute myocarditis, confirmed by CMR as defined by the Lake Louise Criteria. Demographic characteristics and findings from LGE and parametric T1 and T2 mapping were systematically recorded based on chart review with clinical adjudication. This study was approved by the Hamad Medical Corporation Institutional Review Board.

### 2.2. Exposure

The exposure of interest was inflammation as assessed by LGE and myocardial edema from T2 mapping. Inflammation by LGE and edema from T2 were binary variables as assessed by an expert radiologist, while T1 and T2 parametric maps were quantized into eleven and five categories, respectively.

### 2.3. Clinical outcomes

A combined clinical endpoint of cardiac death, arrhythmia (ventricular tachycardia and ventricular fibrillation) and dilated cardiomyopathy (DCM) was used. DCM was identified if left ventricular end diastolic dimension was greater than >117% of age and body surface area and left ventricular ejection fraction <45% both by echocardiography. Patients with pre-existing DCM were excluded from the study [15]. Exploratory analyses were performed with secondary outcomes, including LGE, T2 tissue edema, and T1 and T2 parametric mapping, as they relate to demographics and geographic differences.

### 2.4. CMR acquisition protocol

CMR was performed using 1.5 Tesla scanner (Philips Ingenia, Koninklijke Philips NV 2019, the Netherlands). The CMR protocol consisted of initial localizer sequences coronal and sagittal balanced turbo flash echo (BTFE), axial black blood (BB), cine Images (2chamber, 4chamber, short axis, 3chamber, LV outflow tract, RV outflow tract), T2-weighted BB short axis, spectral presaturation inversion recovery (SPIR) short axis sequences. We also obtained parametric; T2 and T1 mapping images before contrast media administration. Mapping sequences were acquired in 3 slices of short axis orientation. Imaging for post intravenous contrast administration of 0.15 mmol/kg of Gadoterate included early gadolinium sequences and phase-sensitive inversion recovery (PSIR) acquisition for late enhancement.

### 2.5. CMR analysis

Short axis stacks covering base to apex of the entire left ventricle were included in the analysis. Manual volumetric analyses were performed based on steady-state free precession–cine images by experienced investigators using commercially available postprocessing software (IntelliSpace Portal). Analyzed volumetric parameters included LV mass, LV ejection fraction (LVEF), RV ejection fraction (RVEF), end-diastolic volume (EDV), end-systolic volume (ESV), and stroke volume. For manual analyses, LV endo-and epicardial borders and RV endocardial borders were delineated at end-systole and end-diastole. In accordance with current recommendations, the papillary muscles were excluded from the myocardium. T2 SPIR -weighted images short axis sequence was performed used for assessment of the myocardial edema. Early post gadolinium short axis and 4chamber sequences were performed and analyzed for assessment of the myocardial hyperemia. Native T1 and T2 mapping short axis were performed and analyzed for assessment of interstitial myocardial fibrosis and potential myocardial edema. Late post gadolinium enhancement (LGE) short axis, 2-chamber, 3-chamber, and 4-chamber in phase-sensitive inversion recovery (PSIR) acquisition sequences and short axis black blood (BB) sequence were formed and analyzed for assessment of myocardial scar/fibrosis. Diagnosis of myocarditis was made based on at least if 2 out of the 3 Lake Louise criteria were met, (a) regional or global myocardial signal intensity increase on T2 SPIR-weighted images, (b) increased global myocardial early gadolinium enhancement ratio, (c) at least one focal, non-ischemic lesion at inversion recovery LGE .

### 2.6. Statistical analysis

Continuous parameters are presented as mean ± standard deviation (SD) or median and interquartile range (IQR), depending on normality, as assessed by a Shapiro-Wilkes test. Categorical variables are presented as frequencies and percentages. A total of 20 countries were considered in the analysis. To allow for sufficient power for regional variations in CMR inflammation parameters, countries were divided into 6 broad geographical regions: (1) Africa (Sudan, Egypt, other African countries), (2) Southern Asia (Bangladesh, Nepal, India, Sri Lanka, Pakistan, Iran), (3) Western Asia (Lebanon, Iraq, Syria, Qatar, Jordan, Yemen, other countries in the Gulf Cooperation Council), (4) Philippines, (5) US, UK, Canada, and Europe, and (6) Other. Group comparisons for gender and geographical location were performed with a non-parametric Mann-Whitney *U* test, Kruskal Wallis test with Dunn's multiple comparisons, or chi-squared test, where appropriate. Multivariable logistic regression was performed between T2 edema and regions of LGE enhancement and age, gender, body surface area (BSA), and geographical region as defined above.

To agnostically quantify patterns of CMR inflammation in our cohort, Bayesian factor analysis and unsupervised machine learning were used. To account for missingness, a multivariate imputer where each missing values is modeled as a function of other features in a round-robin fashion. The imputer was implemented using the Python SciKit Learn package. All LGE inflammation patterns, T2 edema, and T1 and T2 parametric maps were considered for factor analysis. Parameters for factor analysis are detailed as follows: A tolerance of 0.01 was used for

convergence, with a maximum of 1000 iterations. A vector of ones was used for noise variance initialization. A randomized algorithm was used for singular value decomposition with 3 iterations for the power method. For all analysis, two low dimensional latent factors were considered. Following factor analysis, the original untransformed data were fit with a K Means classifier, a method for unsupervised machine learning. Briefly, K Means assigns each patient one of three clusters depending on which centroid it is closest to in n-dimensional space. The algorithm was implemented using the Python SciKit Learn package with default parameters. The optimum number of clusters was determined by determining which maximized the silhouette score. Group comparisons between clusters were performed using a non-parametric Mann-Whitney *U* test or chi-squared test, where appropriate. All machine learning and factor analysis protocols were implemented in Python, and all statistical analysis were performed using Stata/SE 15.1 (StataCorp LLC, College Station, TX). A P value $< 0.05$ was considered statistically significant.

## 3. Results

### 3.1. Study population

Of 169 consecutive acute myocarditis patients in our study, all patients in our cohort had LGE and qualitative assessment of edema on T2. A total of 41/169 (24%) and 45/169 (27%) had T1 and T2 mapping performed, respectively. Summary patient characteristics, and characteristics stratified by a combined clinical endpoint of cardiac death, arrythmia, and DCM are shown in Table 1. The median (IQR) age was 36 yrs. (29–46 yrs.), and 22% were women. Our cohort was racially and ethnically diverse with 25% from Northern Africa, 33% from Southern Asia, and 28% from Western Asia/the Middle East. All 169 patients had a primary diagnosis of acute myocarditis and 5% had a secondary diagnosis of DCM. Only 3/169 (2%) of all patients in the cohort had endomyocardial biopsy confirmed myocarditis. Viral panels for cytomegalovirus (CMV)/Epstein-Barr Virus (EBV), Hepatitis B virus (HBV) core and surface antibody and surface antigen, and influenza virus B was performed. Briefly, 2 patients were positive for CMV, 2 for EBV, 2 had positive HBV surface antigen, and 2 were positive for influenza type B virus. Computed tomography coronary angiography was performed in 37% of patients, with 2% showing significant coronary occlusion. Invasive angiography was performed in 38% patients, with 10% showing significant coronary occlusion. Twelve patients met the combined clinical endpoint – 3 had arrythmia, 8 had DCM, and 1 died. Of these, 2 patients had significant coronary occlusion. Additionally, 11 (7%) of patients had a >10% improvement in ejection fraction during hospitalization, 16 (9%) had a >20% or complete normalization in ejection fraction, and 98 (58%) were asymptomatic.

### 3.2. Comparison of LGE patterns by clinical endpoint

We first assessed patterns of LGE inflammation and T1 and T2 parametric maps between those patients that met the combined clinical endpoint and those that did not (Table 1). We found higher left ventricular (LV) systolic ($p < 0.001$) and diastolic ($p < 0.001$) volumes and reduced LV ejection fraction $P = 0.034$) in patients that met the combined endpoint. Right ventricular ejection fraction was reduced in patients that met the combined endpoint but not significantly ($p = 0.057$). Furthermore, in those patients with events, there was anterior ($p = 0.034$), septal ($p = 0.042$), and subendocardial ($p = 0.001$) LGE.

### 3.3. Comparison of LGE patterns by geography

We then performed sub-group analysis in LGE parameters by geography (**Supplemental Table S1**) and gender (**Supplemental Table S2**). We found that LGE and T1 and T2 parametric maps were not significantly different among the 6 broad geographic regions we studied. However, we found that females in our cohort were more likely to less

**Table 1**
Baseline characteristics of acute myocarditis patients with LGE, T1, and T2 maps. Demographic characteristic and CMR characteristics, including LGE, T1, and T2 maps, are shown. BSA – Body Surface Area; CMR – Cardiovascular Magnetic Resonance; LVEDVi – Left Ventricular End Diastolic Volume indexed; LVESVi – Left Ventricular End Systolic Volume indexed; LVEF – Left Ventricular Ejection Fraction; RVEF – Right Ventricular Ejection Fraction; LGE – Late Gadolinium Enhancement; T1 – Spin-lattice relaxation; T2 – Transverse relaxation; Hs – High-Sensitivity; CRP – C Reactive Protein.

| Summary Characteristics | All Participants (n = 169) | Events (n = 12) | No Events (n = 131) | P Value |
|---|---|---|---|---|
| Age | 38 ± 13 | 43 ± 13 | 37 ± 13 | 0.1456 |
| Gender, (% Men) | 78% | 83% | 72% | 0.529 |
| Height, cm | 168 ± 8 | 170 ± 7 | 168 ± 9 | 0.3193 |
| Weight, kg | 78 ± 17 | 76 ± 17 | 78 ± 17 | 0.9121 |
| BSA, $m^2$ | 2.3 ± 5.9 | 2 ± 0.2 | 2 ± 7 | 0.7519 |
| Region | | | | 0.757 |
| Africa | 42 (25%) | 4 (33%) | 31 (24%) | |
| Southern Asia | 55 (33%) | 2 (17%) | 41 (31%) | |
| UK, US, Europe, Canada | 10 (6%) | 0 (0%) | 4 (3%) | |
| Western Asia | 47 (28%) | 5 (42%) | 39 (30%) | |
| Philippines | 9 (5%) | 1 (8%) | 6 (5%) | |
| Others | 6 (3%) | 0 (0%) | 4 (3%) | |
| CMR LVEDVi | | | | **<0.001** |
| <50 | 12 (7%) | 0 (0%) | 11 (8%) | |
| 51–60 | 26 (15%) | 1 (8%) | 21 (16%) | |
| 61–70 | 37 (22%) | 1 (8%) | 29 (22%) | |
| 71–80 | 28 (17%) | 0 (0%) | 22 (17%) | |
| 81–90 | 23 (14%) | 0 (0%) | 21 (16%) | |
| 101–110 | 16 (9%) | 6 (50%) | 8 (6%) | |
| 111–120 | 3 (2%) | 0 (0%) | 2 (2%) | |
| 121–130 | 5 (3%) | 1 (8%) | 1 (0.8%) | |
| 141–150 | 1 (1%) | 1 (8%) | 0 (0%) | |
| >151 | 4 (2%) | 1 (8%) | 3 (2%) | |
| CMR LVESVi | | | | **<0.001** |
| <50 | 124 (73%) | 3 (25%) | 98 (78%) | |
| 51–60 | 9 (5%) | 0 (0%) | 7 (6%) | |
| 61–70 | 9 (5%) | 3 (25%) | 6 (5%) | |
| 71–80 | 6 (4%) | 0 (0%) | 5 (4%) | |
| 81–90 | 4 (3%) | 1 (8%) | 3 (2%) | |
| 91–100 | 5 (3%) | 1 (8%) | 2 (2%) | |
| 101–110 | 8 (5%) | 4 (33%) | 0 (0%) | |
| 111–120 | 1 (1%) | 0 (0%) | 1 (0.8%) | |
| >120 | 3 (2%) | – | – | |
| CMR LVEF, % | | | | **0.034** |
| <15 | 2 (1%) | 1 (8%) | 1 (0.8%) | |
| 16–25 | 13 (8%) | 2 (17%) | 5 (4%) | |
| 26–35 | 14 (8%) | 2 (17%) | 11 (9%) | |
| 36–45 | 15 (9%) | 2 (17%) | 11 (9%) | |
| 46–55 | 40 (24%) | 3 (25%) | 30 (24%) | |
| >56 | 85 (50%) | 2 (17%) | 67 (54%) | |
| CMR RVEF, % | | | | 0.057 |
| <15 | 1 (1%) | 0 (0%) | 1 (0.8%) | |
| 16–25 | 5 (3%) | 2 (17%) | 2 (2%) | |
| 26–35 | 10 (6%) | 1 (8%) | 5 (4%) | |
| 36–45 | 20 (12%) | 2 (17%) | 11 (9%) | |
| 46–55 | 70 (41%) | 4 (33%) | 58 (46%) | |
| >56 | 63 (37%) | 3 (25%) | 48 (38%) | |
| LGE | | | | |
| Edema/T2, % | 64 (38%) | 0 (0%) | 48 (38%) | **0.008** |
| Early Gad, % | 7 (4%) | 1 (8%) | 4 (3%) | 0.365 |
| LGE/Anterior, % | 41 (24%) | 6 (50%) | 28 (22%) | **0.034** |
| LGE/Septal, % | 58 (34%) | 7 (58%) | 37 (30%) | **0.042** |
| LGE/Inferior, % | 93 (55%) | 8 (67%) | 28 (58%) | 0.578 |
| LGE/Lateral, % | 124 (73%) | 8 (67%) | 93 (74%) | 0.561 |
| LGE Sub-epicardial, % | 99 (59%) | 8 (67%) | 71 (57%) | 0.509 |
| LGE Mid-wall, % | 101 (60%) | 7 (58%) | 81 (65%) | 0.655 |
| LGE Sub-endocardial, % | 12 (7%) | 3 (25%) | 4 (3%) | **0.001** |
| T1 Map | | | | 0.991 |
| <890 | 13 (8%) | 1 (8%) | 12 (7%) | |
| 891–910 | 1 (1%) | 0 (0%) | 1 (0.8%) | |
| 911–930 | 1 (1%) | 0 (0%) | 1 (0.8%) | |
| 951–970 | 2 (1%) | 0 (0%) | 2 (2%) | |
| 971–990 | 2 (1%) | 0 (0%) | 1 (0.8%) | |
| 991–1010 | 4 (2%) | – | – | |
| 1011–1030 | 4 (2%) | 0 (0%) | 3 (2%) | |
| 1051–1070 | 6 (4%) | 0 (0%) | 6 (5%) | |

(*continued on next page*)

**Table 1** (*continued*)

| Summary Characteristics | All Participants (n = 169) | Events (n = 12) | No Events (n = 131) | P Value |
|---|---|---|---|---|
| 1071–1090 | 2 (1%) | 0 (0%) | 2 (2%) | |
| 1091–1110 | 1 (1%) | 0 (0%) | 1 (0.8%) | |
| >1111 | 5 (3%) | 0 (0%) | 4 (3%) | |
| T2 Map | | | | 0.558 |
| <40 | 11 (7%) | 1 (8%) | 10 (8%) | |
| 46–50 | 10 (6%) | 0 (0%) | 8 (6%) | |
| 51–55 | 12 (7%) | 0 (0%) | 10 (8%) | |
| 56–60 | 3 (2%) | 0 (0%) | 3 (2%) | |
| >61 | 9 (5%) | 0 (0%) | 9 (7%) | |
| Peak Hs Troponin | | | | 0.127 |
| <15 | 34 (20%) | 1 (8%) | 30 (24%) | |
| 15–50 | | | | |
| 51–100 | 7 (4%) | 0 (0%) | 7 (6%) | |
| 101–300 | 17 (10%) | 1 (8%) | 14 (11%) | |
| 301–500 | 13 (8%) | 1 (8%) | 10 (8%) | |
| 501–1000 | 14 (8%) | 0 (0%) | 9 (7%) | |
| >1000 | 27 (16%) | 0 (0%) | 15 (12%) | |
| CRP | | | | 0.613 |
| 21–50 | 21 (12%) | 0 (0%) | 16 (13%) | |
| 5–20 | 27 (16%) | 2 (17%) | 23 (18%) | |
| 51–100 | 9 (5%) | 0 (0%) | 6 (5%) | |
| <5 | 40 (24%) | 4 (33%) | 30 (24%) | |
| >100 | 7 (4%) | 0 (0%) | 5 (4%) | |

anterior (p = 0.001), inferior (p = 0.002), lateral (p = 0.035), and sub-epicardial (p = 0.004) LGE, suggesting a unique pattern of inflammation different from what is commonly reported. Following this analysis, we performed multivariable logistic regression with LGE inflammation parameters predicted by geography and adjusting for age, gender, and BSA (Table 2). In this analysis, we found that gender is independently associated with T2 edema (p = 0.031) and anterior and inferior (p = 0.002) LGE. We further found that southern (p = 0.041) and western (p = 0.043) Asian patients were independently associated with have lateral LGE, while patients from Western countries were independent associated with mid-wall LGE (p = 0.049).

### 3.4. Agnostic determination of LGE patterns

Next, we sought to agnostically identify patterns of LGE and T1 and T2 parametric maps using machine learning. Using *only* the location of LGE and the magnitude of T1 and T2 in the myocardium, we performed factor analysis. The objective of factor analysis is to identify whether a smaller subset of latent factors is sufficient to explain the variance in the data. For low-dimensional representation, we utilized two factors, as shown in Fig. 1. As shown, geographical differences do not align with any one factor (Fig. 1**A**). Female gender appears to align with a positive value for Factor 2, consistent with our results from multivariable logistic regression (Fig. 1**B**). Furthermore, 9/12 patients who met the total combined endpoint were found to have a negative value for Factor 1, while only 3/12 had a positive value (Fig. 1**C**).Fig. 2..

We next performed K means clustering, a form of unsupervised machine learning, to identify clusters of inflammation using LGE and T1 and T2 parametric maps. To determine the optimal number of clusters for our dataset, we utilized a silhouette score, which is the ratio between the mean intra-cluster distance and nearest cluster distance. We found that two clusters maximized the silhouette score, cluster 1 with n = 31 patients and cluster 2n = 106 patients. We then utilized factor analysis for low dimensional data representation of our clusters followed by sub-group analysis of LGE parameters (Table 3). Here, we found that patients in cluster 2 had more T2 edema (p < 0.001) and increased anterior (p < 0.001) and sup-epicardial (p = 0.011) LGE. On the other hand, T1 (p < 0.001) and T2 (p < 0.001) values in myocardium from parametric mapping were elevated in cluster 1, further highlighting the differences between these clusters.

**Table 2**
Multivariable Logistic Regression of LGE inflammation and patient geographic and demographic characteristics. Shown here are the odds ratios (OR) with 95% confidence intervals (CI) and P-values for each combinations of independent variables (rows) and a dependent variables (columns). For the region covariate, general linear mixed models were constructed in reference to patients from Africa. P < 0.05 was considered significant. LGE – Late Gadolinium Enhancement; T1 – Spin-lattice relaxation; T2 – Transverse relaxation; Gad – Gadolinium; NA, Not Applicable. * ORs for these combinations could not be calculated.

| Variable | Model | | | | | | | | |
|---|---|---|---|---|---|---|---|---|---|
| | Edema T2 | EGE | LGE anterior | LGE septal | LGE inferior | LGE lateral | LGE subepicardial | LGE midwall | LGE subendocardial |
| **Age** | 0.99 (0.96–1.01), p = 0.260 | 0.99 (0.92–1.05), p = 0.665 | 1.01 (0.98–1.04), p = 0.627 | 1.01 (0.99–1.04), p = 0.321 | 1.00 (0.98–1.03), p = 0.808 | 1.00 (0.97–1.03), p = 0.854 | 0.98 (0.96–1.01), p = 0.157 | 0.98 (0.96–1.01), p = 0.128 | 1.04 (0.99–1.09), p = 0.156 |
| **Female** | **0.35 (0.13–0.91), p = 0.031** | NA* | **0.07 (0.01–0.51), p = 0.009** | 0.44 (0.16–1.20), p = 0.110 | **0.26 (0.11–0.62), p = 0.002** | 0.49 (0.18–1.36), p = 0.171 | 0.43 (0.17–1.08), p = 0.073 | 0.70 (0.28–1.78), p = 0.460 | 0.51 (0.07–3.64), p = 0.503 |
| **BSA** | 1.09 (0.65–1.82), p = 0.754 | 0.31 (0.00–36.89), p = 0.631 | 1.07 (0.82–1.41), p = 0.609 | 0.77 (0.10–5.72), p = 0.796 | 1.06 (0.80–1.40), p = 0.706 | 1.66 (0.17–16.62), p = 0.666 | 1.99 (0.28–14.24), p = 0.491 | 2.06 (0.28–15.13), p = 0.479 | 0.36 (0.01–20.18), p = 0.618 |
| **Region** | | | | | | | | | |
| — Philippines | 0.79 (0.14–4.56), p = 0.796 | NA* | NA* | 1.67 (0.35–8.03), p = 0.520 | 2.99 (0.59–15.23), p = 0.187 | 0.53 (0.07–3.91), p = 0.536 | 0.86 (0.18–4.15), p = 0.851 | 7.12 (0.75–67.83), p = 0.088 | NA* |
| — Southern Asia | 1.58 (0.66–3.76), p = 0.302 | 0.60 (0.06–5.98), p = 0.664 | 1.67 (0.64–4.38), p = 0.296 | 1.08 (0.41–2.81), p = 0.882 | 1.28 (0.55–2.97), p = 0.560 | **0.26 (0.07–0.94), p = 0.041** | 1.29 (0.50–3.36), p = 0.602 | 1.18 (0.45–3.05), p = 0.738 | 0.96 (0.20–4.54), p = 0.956 |
| — UK, US, Europe, Canada | 1.72 (0.42–7.04), p = 0.451 | NA* | 1.31 (0.28–6.16), p = 0.734 | 0.42 (0.08–2.30), p = 0.320 | 0.76 (0.19–3.05), p = 0.698 | **0.13 (0.02–0.68), p = 0.016** | 0.81 (0.19–3.39), p = 0.769 | **0.22 (0.05–1.00), p = 0.049** | NA* |
| — Western Asia | 1.43 (0.57–3.57), p = 0.447 | 1.17 (0.15–9.01), p = 0.880 | 1.43 (0.50–4.14), p = 0.508 | 0.82 (0.33–2.06), p = 0.672 | 1.45 (0.60–3.55), p = 0.410 | **0.28 (0.08–0.96), p = 0.043** | 1.31 (0.53–3.23), p = 0.561 | 1.05 (0.43–2.57), p = 0.909 | NA* |
| — Others | 1.40 (0.21–9.29), p = 0.727 | 7.86 (0.46–134.45), p = 0.155 | 1.35 (0.12–15.54), p = 0.812 | 1.17 (0.18–7.76), p = 0.870 | 0.70 (0.10–4.70), p = 0.713 | **0.07 (0.01–0.54), p = 0.011** | 0.48 (0.07–3.14), p = 0.440 | 0.37 (0.06–2.39), p = 0.296 | 2.18 (0.18–27.14), p = 0.544 |

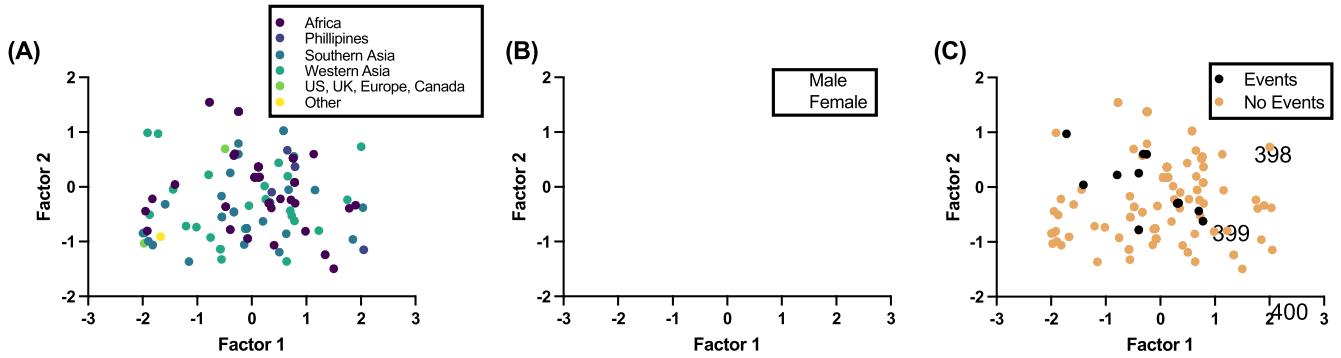


**Fig. 1.** Factor analysis of LGE inflammation and T1 and T2 parametric mapping data in acute myocarditis. We represented patterns of inflammation using two latent factors. Plots are shown after color-coding for (A) geography, (B) gender, and (C) events. Events in our analysis included arrhythmia, dilated cardiomyopathy, or death. LGE – Late Gadolinium Enhancement; T1 – Spin-lattice relaxation; T2 – Transverse relaxation.

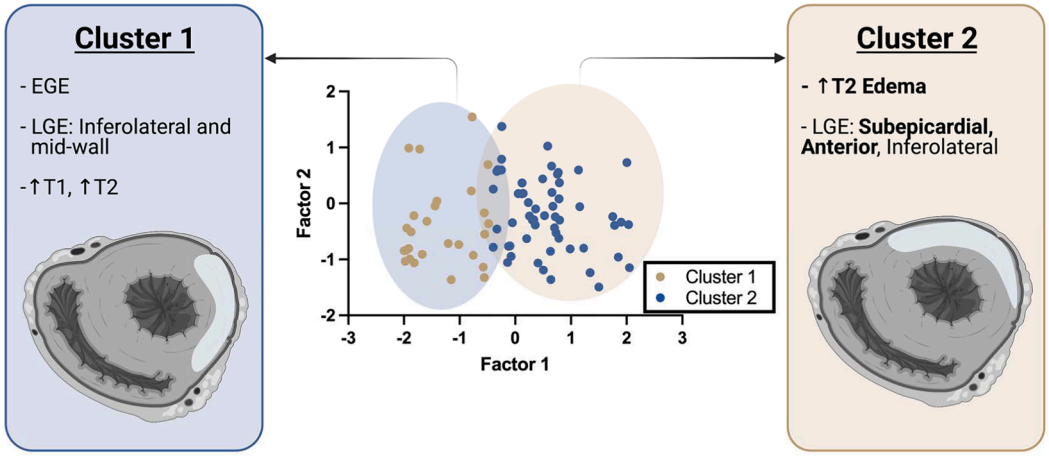


**Fig. 2.** Machine learning identified two predominant clusters of LGE and T1 and T2 parametric mapping. Using K Means clustering, we found two clusters best fit our cohort as assessed by a silhouette score. Based on sub-group analysis (Table 3), cluster 1 (left) was found to have more EGE, increased inferolateral and mid-wall LGE, and increased T1 and T2. On the other hand, cluster 2 (right) was found to have increased T2 edema and subepicardial, anterior, and inferolateral LGE. EGE – Early Gadolinium Enhancement; LGE – Late Gadolinium Enhancement; T1 – Spin-lattice relaxation; T2 – Transverse relaxation.

## 4. Discussion

The present investigation describes patterns of LGE inflammation and T1/T2 parametric maps in a cohort of 169 CMR confirmed acute myocarditis patients. The principal findings from out study are as follows: (1) patients with worsened outcomes, defined here as arrhythmia, DCM, or death, had dilated ventricles (provided DCM is included as an end point), depressed LV systolic function, and increased anterior/septal LGE; (2) geographical differences do not underlie differences in patterns of CMR inflammation; (3) female patients, however, were less likely to have T2 edema and sub-epicardial inferolateral inflammation, suggesting a deviation from classic patterns of CMR inflammation in acute myocarditis; (4) unsupervised machine learning in conjunction with factor analysis identified two predominant patterns of CMR inflammation, each with distinct features (**Central Illustration**). In cluster 2 (n = 106), patients were more likely to have EGE, inferolateral and mid-wall LGE, and increased myocardial T1/T2 from parametric mapping. In cluster 1 (n = 31), patients had increased T2 edema and increased subepicardial anterior and inferolateral LGE. The present study thus agnostically identifies clusters of myocardial inflammation from CMR in a racially and ethnically diverse group of patients from Southern Asia, Northern Africa, and the Middle East.

In Western populations, two primary patterns of inflammation from CMR have been identified in acute myocarditis, namely subepicardial inferolateral LGE and mid-wall anteroseptal LGE [5,16]. The pattern of inflammation in acute myocarditis has been shown to have prognostic and functional significance. Indeed, the ITalian multicenter study on Acute Myocarditis (ITAMY) study found that patients with predominant anteroseptal inflammation by LGE had a worse prognosis than other groups and that this pattern of inflammation was the best predictor of their combined endpoint, which consisted of cardiac death, implantable cardioverter-defibrillator firing, heart failure hospitalization, and resuscitation cardiac arrest [16]. Furthermore, a study by Li et al. found that patients with predominant anteroseptal LGE had worsened LV ejection fractions [9]. However, these studies are restricted to centers in Europe. Our study confirmed in a different geographic population from Southern Asia, Northern Africa, and the Middle East that anteroseptal inflammation still predicts worsened outcomes. Whether similarities in etiology of viral myocarditis contributes to these findings are of interest for future investigations.

Despite several studies highlighting that difference etiologies of myocarditis are hypothesized to elicit different patterns of inflammation on CMR [11,13,14], we found that geography failed to account for the variance in CMR inflammation in our cohort. We did however find that female patients had a unique pattern of CMR inflammation disparate from males and more importantly, the classic subepicardial inferolateral LGE observed in myocarditis [4]. Small animal models have found a polarized response to myocarditis Coxsackivirus Type B infection, though such a dimorphism has not been shown in humans [17]. In subgroup analysis, we found that female patients were less likely to have T2

**Table 3**
Patient and CMR characteristics of Patients with Acute Myocarditis according to machine learning derived cluster and Bayesian factor analysis. In the cohort, each patient was assigned to one of two clusters identified by K means clustering, a method of unsupervised machine learning. Characteristics were compared with either a Mann-Whitney *U* test or Chi-Squared test, where appropriate. BSA – Body Surface Area; CMR – Cardiovascular Magnetic Resonance; LVEDVi – Left Ventricular End Diastolic Volume indexed; LVESVi – Left Ventricular End Systolic Volume indexed; LVEF – Left Ventricular Ejection Fraction; RVEF – Right Ventricular Ejection Fraction; LGE – Late Gadolinium Enhancement; T1 – Spin-lattice relaxation; T2 – Transverse relaxation; Hs – High-Sensitivity; CRP – C Reactive Protein.

| Summary Characteristics | Cluster 1 (n = 31) | Cluster 2 (n = 106) | P-Value |
|---|---|---|---|
| Gender, (% Men) | 27, (87%) | 77, (73%) | 0.098 |
| Height, cm | 170 ± 9 | 168 ± 8 | 0.1123 |
| Weight, kg | 82 ± 15 | 77 ± 17 | 0.0949 |
| BSA, $m^2$ | 4 ± 14 | 2 ± 0.2 | **0.0351** |
| Age, yrs | 36 ± 12 | 39 ± 14 | 0.2832 |
| Region | | | 0.477 |
| Africa | 7 (23 %) | 28 (26 %) | |
| Southern Asia | 9 (29 %) | 34 (32%) | |
| UK, US, Europe, Canada | 2 (6%) | 2 (2%) | |
| Western Asia | 12 (39%) | 32 (30%) | |
| Others | 1 (3 %) | 3 (3%) | |
| CMR LVEDVi | | | 0.354 |
| <50 | 3 (10 %) | 8 (8%) | |
| 51–60 | 7 (23%) | 15 (14%) | |
| 61–70 | 6 (19%) | 24 (23 %) | |
| 71–80 | 7 (23%) | 15 (14%) | |
| 81–90 | 2 (6%) | 19 (18%) | |
| 101–110 | 2 (6%) | 12 (11%) | |
| 111–120 | 1 (3%) | 1 (0.9%) | |
| 121–130 | 0 (0%) | 2 (2%) | |
| 141–150 | 1 (3%) | 0 (0%) | |
| >151 | 0 (0%) | 4 (4%) | |
| CMR LVESVi | | | 0.433 |
| <50 | 25 (81%) | 76 (72%) | |
| 51–60 | 0 (0%) | 7 (7%) | |
| 61–70 | 4 (13%) | 5 (5%) | |
| 71–80 | 1 (3%) | 4 (4%) | |
| 81–90 | 0 (0%) | 4 (4%) | |
| 91–100 | 0 (0%) | 3 (3%) | |
| 101–110 | 1 (3%) | 3 (3%) | |
| 111–120 | 0 (0%) | 1 (0.9%) | |
| CMR LVEF, % | | | 0.160 |
| <15 | 0 (0%) | 2 (2%) | |
| 16–25 | 0 (0%) | 7 (7%) | |
| 26–35 | 0 (0%) | 13 (12%) | |
| 36–45 | 4 (13%) | 9 (8%) | |
| 46–55 | 8 (26%) | 25 (24%) | |
| >56 | 19 (61%) | 50 (47%) | |
| CMR RVEF, % | | | 0.207 |
| <15 | 0 (0%) | 1 (0.9%) | |
| 16–25 | 0 (0%) | 4 (4%) | |
| 26–35 | 0 (0%) | 6 (6%) | |
| 36–45 | 1 (3%) | 12 (11%) | |
| 46–55 | 19 (61%) | 43 (41%) | |
| >56 | 11 (35%) | 40 (38%) | |
| LGE | | | |
| Edema/T2, % | 23 (74%) | 25 (24%) | **<0.001** |
| Early Gad, % | 0 (0%) | 5 (5%) | 0.218 |
| LGE/Anterior, % | 16 (52%) | 18 (17%) | **<0.001** |
| LGE/Septal, % | 10 (32%) | 34 (32%) | 0.985 |
| LGE/Inferior, % | 21 (68%) | 60 (57%) | 0.267 |
| LGE/Lateral, % | 25 (81%) | 76 (72%) | 0.319 |
| LGE Sub-epicardial, % | 24 (77%) | 55 (52%) | **0.011** |
| LGE Mid-wall, % | 17 (55%) | 71 (67%) | 0.215 |
| LGE Sub-endocardial, % | 2 (6%) | 5 (5%) | 0.700 |
| T1 Map | | | **<0.001** |
| <890 | 13 (42%) | 0 (0%) | |
| 891–910 | 1 (3%) | 0 (0%) | |
| 911–930 | 1 (3%) | 0 (0%) | |
| 951–970 | 2 (6%) | 0 (0%) | |
| 971–990 | 0 (0%) | 1 (0.9%) | |
| 1011–1030 | 0 (0%) | 3 (3%) | |
| 1051–1070 | 0 (0%) | 6 (6%) | |
| 1071–1090 | 0 (0%) | 2 (2%) | |
| 1091–1110 | 0 (0%) | 1 (0.9%) | |
| >1111 | 0 (0%) | 4 (4%) | |
| T2 Map | | | **<0.001** |
| <40 | 9 (8%) | 2 (2%) | |
| 46–50 | 4 (15%) | 4 (4%) | |
| 51–55 | 0 (0%) | 10 (9%) | |
| 56–60 | 0 (0%) | 3 (3%) | |
| >61 | 1 (4%) | 8 (8%) | |

edema and sub-epicardial inferolateral inflammation. To our knowledge, ours was the first study to identify a unique pattern of inflammation in female patients from non-European countries with acute myocarditis. Future studies are required to identify the prognostic significance of this finding.

The recent updates in 2018 to the LLC highlight the value of T1 and T2 parametric mapping for diagnosis and risk stratification of acute myocarditis [6,8,9,18,19]. In our study, we found that machine learning derived clusters resulted in two disparate clusters, one with an anterior and inferolateral pattern of LGE inflammation and the other with increased myocardial T1/T2 from parametric mapping. Furthermore, machine learning failed to identify differences in the cohort without the addition of parametric mapping data, further highlighting its importance in assessing the phenotype of inflammation in myocarditis. Preliminary subgroup analysis appears to suggest that anterior LGE was more associated with worsened outcomes as compared to T1/T2 parametric mapping, potentially suggesting that patients in cluster 2 are in an earlier phase of myocarditis compared to cluster 1 [20,21]. Analysis incorporating more sophisticated measures , including cardiac texture analysis [18,19] and how these relate to subclinical myocardial injury in acute myocarditis, is of future interest.

### 4.1. Limitations

There are a couple of limitations which should be considered. Confirmation of the diagnosis of acute myocarditis by endomyocardial biopsy was only obtained for 3 patients. Viral reverse transcriptase polymerase chain reaction tests only confirmed a clear etiology in 9 patients in our cohort. Our study only had 12 patients who experienced a cardiac event, making much of our analysis under-powered for more detailed statistical testing. As such, statistical comparisons from factor analysis were under-powered. These findings are consistent with the event rate in acute myocarditis overall but nonetheless affect the analysis. All CMR studies were conducted at single site. T1 and T2 parametric maps were only obtained for a subset of patients. While missingness was accounted for by iterative imputation, generalizability of the results from our model may be limited. Future studies should aim to validate the models in larger cohorts across multiple sites.

## 5. Conclusion

In a cohort of 169 CMR confirmed acute myocarditis patients from Northern Africa, Asia, and the Middle East, we assessed whether different patterns of LGE inflammation and myocardial T1 and T2 are associated with specific gender, geography, and cardiac events. Consistent with prior studies, we found that anteroseptal inflammation is associated with worsened outcomes. We further identified that female patients in our cohort are less likely to have the classic pattern of sub-epicardial inferolateral LGE observed in European countries. Finally, using machine learning in combination with factor analysis, we agnostically identified two clusters. In cluster 1, patients were more likely to have EGE, inferolateral and mid-wall LGE, and increased myocardial

T1/T2 from parametric mapping. In cluster 2, patients had increased T2 edema and increased sub-epicardial anterior and inferolateral LGE. Future studies should be aimed to validate both our findings and our approach in a larger cohort with a similar racial and ethnic composition.

## Declaration of Competing Interest

The authors declare that they have no known competing financial interests or personal relationships that could have appeared to influence the work reported in this paper.

## Acknowledgement

J. Van den Eynde was supported by a Fellowship of the Belgian American Educational Foundation.

## Appendix A. Supplementary material

Supplementary data to this article can be found online at https://doi.org/10.1016/j.ijcha.2022.101029.

## References

[1] G.A. Roth, G.A. Mensah, C.O. Johnson, G. Addolorato, E. Ammirati, L.M. Baddour, N.C. Barengo, A.Z. Beaton, E.J. Benjamin, C.P. Benziger, Global burden of cardiovascular diseases and risk factors, 1990–2019: update from the GBD 2019 study, J. Am. Coll. Cardiol. 76 (25) (2020) 2982–3021.
[2] L.T. Cooper Jr, Myocarditis, N. Engl. J. Med. 360 (15) (2009) 1526–1538.
[3] H.T. Aretz, Myocarditis: the Dallas criteria, Hum. Pathol. 18 (6) (1987) 619–624.
[4] M.P. Gannon, E. Schaub, C.L. Grines, S.G. Saba, State of the art: evaluation and prognostication of myocarditis using cardiac MRI, J. Magn. Reson. Imaging 49 (7) (2019) e122–e131.
[5] H. Mahrholdt, C. Goedecke, A. Wagner, G. Meinhardt, A. Athanasiadis, H. Vogelsberg, P. Fritz, K. Klingel, R. Kandolf, U. Sechtem, Cardiovascular Magnetic Resonance Assessment of Human Myocarditis, Circulation 109 (10) (2004) 1250–1258.
[6] M. Gutberlet, B. Spors, T. Thoma, H. Bertram, T. Denecke, R. Felix, M. Noutsias, H.-P. Schultheiss, U. Kühl, Suspected Chronic Myocarditis at Cardiac MR: Diagnostic Accuracy and Association with Immunohistologically Detected Inflammation and Viral Persistence, Radiology 246 (2) (2008) 401–409.
[7] J.-P. Laissy, B. Messin, O. Varenne, B. Iung, D. Karila-Cohen, E. Schouman-Claeys, P.G. Steg, MRI of acute myocarditis: a comprehensive approach based on various imaging sequences, Chest 122 (5) (2002) 1638–1648.
[8] C. Liguori, D. Farina, F. Vaccher, G. Ferrandino, D. Bellini, I. Carbone, Myocarditis: imaging up to date, Radiol. Med. (Torino) 125 (11) (2020) 1124–1134.
[9] H. Li, H. Zhu, Z. Yang, D. Tang, L. Huang, L. Xia, Tissue Characterization by Mapping and Strain Cardiac MRI to Evaluate Myocardial Inflammation in Fulminant Myocarditis, J. Magn. Reson. Imaging 52 (3) (2020) 930–938.
[10] S.V. Raman, Y. Siddiqui, Mapping myocarditis: still searching for the North Star, American College of Cardiology Foundation Washington, DC, 2014.
[11] V.M. Ferreira, J. Schulz-Menger, G. Holmvang, C.M. Kramer, I. Carbone, U. Sechtem, I. Kindermann, M. Gutberlet, L.T. Cooper, P. Liu, M.G. Friedrich, Cardiovascular Magnetic Resonance in Nonischemic Myocardial Inflammation, J. Am. Coll. Cardiol. 72 (24) (2018) 3158–3176.
[12] J.A. Luetkens, A. Faron, A. Isaak, D. Dabir, D. Kuetting, A. Feisst, F.C. Schmeel, A. M. Sprinkart, D. Thomas, Comparison of original and 2018 Lake Louise criteria for diagnosis of acute myocarditis: results of a validation cohort, Radiology: Cardiothoracic, Imaging 1 (3) (2019), e190010.
[13] M. Jeserich, E. Brunner, R. Kandolf, M. Olschewski, S. Kimmel, M.G. Friedrich, D. Föll, C. Bode, A. Geibel, Diagnosis of viral myocarditis by cardiac magnetic resonance and viral genome detection in peripheral blood, Int. J. Cardiovasc. Imaging 29 (1) (2013) 121–129.
[14] P. Lurz, I. Eitel, J. Adam, J. Steiner, M. Grothoff, S. Desch, G. Fuernau, S. de Waha, M. Sareban, C. Luecke, Diagnostic performance of CMR imaging compared with EMB in patients with suspected myocarditis, JACC: Cardiovasc. Imaging 5 (5) (2012) 513–524.
[15] P. Rubis, The diagnostic work up of genetic and inflammatory dilated cardiomyopathy, E-J. Cardiol. Practice 13 (2015).
[16] G.D. Aquaro, M. Perfetti, G. Camastra, L. Monti, S. Dellegrottaglie, C. Moro, A. Pepe, G. Todiere, C. Lanzillo, A. Scatteia, M.D. Roma, G. Pontone, M.P. Marra, A. Barison, G.D. Bella, Cardiac MR With Late Gadolinium Enhancement in Acute Myocarditis With Preserved Systolic Function, J. Am. Coll. Cardiol. 70 (16) (2017) 1977–1987.
[17] K. Li, W. Xu, Q. Guo, Z. Jiang, P. Wang, Y. Yue, S. Xiong, Differential macrophage polarization in male and female BALB/c mice infected with coxsackievirus B3 defines susceptibility to viral myocarditis, Circ. Res. 105 (4) (2009) 353–364.
[18] B. Baessler, C. Luecke, J. Lurz, K. Klingel, A. Das, M. von Roeder, S. de Waha-Thiele, C. Besler, K.-P. Rommel, D. Maintz, Cardiac MRI and texture analysis of myocardial T1 and T2 maps in myocarditis with acute versus chronic symptoms of heart failure, Radiology 292 (3) (2019) 608–617.
[19] B. Baessler, C. Luecke, J. Lurz, K. Klingel, M. von Roeder, S. de Waha, C. Besler, D. Maintz, M. Gutberlet, H. Thiele, Cardiac MRI texture analysis of T1 and T2 maps in patients with infarctlike acute myocarditis, Radiology 289 (2) (2018) 357–365.
[20] U.K. Radunski, G.K. Lund, D. Säring, S. Bohnen, C. Stehning, B. Schnackenburg, M. Avanesov, E. Tahir, G. Adam, S. Blankenberg, T1 and T2 mapping cardiovascular magnetic resonance imaging techniques reveal unapparent myocardial injury in patients with myocarditis, Clin. Res. Cardiol. 106 (1) (2017) 10–17.
[21] R. Hinojar, E. Nagel, V.O. Puntmann, T1 mapping in myocarditis–headway to a new era for cardiovascular magnetic resonance, Expert Rev. Cardiovasc. Therapy 13 (8) (2015) 871–874.